Progress in Natural Science: Materials International 2013;23(4):382–387

Chinese Materials Research Society

Progress in Natural Science: Materials International

www.elsevier.com/locate/pnsmi
www.sciencedirect.com

ORIGINAL RESEARCH

Structural stability and Raman scattering of CoPt and NiPt hollow nanospheres under high pressure

Xi Shen[a], Qian Sun[b], Jie Zhu[a], Yuan Yao[a], Jing Liu[c], Changqing Jin[a], Richeng Yu[a,*], Rongming Wang[b,]**

[a]*Beijing National Laboratory for Condensed Matter Physics, Institute of Physics, Chinese Academy of Sciences, P.O. Box 603, Beijing 100190, China*
[b]*Department of Physics, Beihang University, Beijing 100191, China*
[c]*Institute of High Energy Physics, Chinese Academy of Sciences, Beijing 100039, China*

Received 8 February 2013; accepted 22 May 2013
Available online 18 July 2013

KEYWORDS

Hollow nanosphere;
Angle dispersive x-ray diffraction;
High pressure Raman;
Density functional theory

Abstract This paper reports that the high pressure *in situ* angle dispersive x-ray diffraction and Raman scattering studies on CoPt and NiPt hollow nanospheres are performed by means of a diamond anvil cell for generating external pressure at room temperature. The crystal structures of both the CoPt and NiP hollow nanospheres keep stable up to about 41 GPa. Moreover, it shows that the hollow nanospheres possess higher bulk moduli than their bulk counterparts by using the first-principles density functional theory.

1. Introduction

In the past several decades, synthetic, structural and property analyses on bimetallic system have caused fundamental and technological interests in diverse applications such as binary catalytic materials [1–3], metal colloid science [4,5] and ultrahigh-density optical and magnetic recording storages [6,7], *etc.* Meanwhile, the bimetallic compounds often reveal enhanced electrocatalytic activities [1] for the oxygen reduction reaction in comparison with their pure metal components, they can adjust finely surface plasma effect [4] associated with the electrochemical process and intrinsic ferromagnetic property [7] by changing the ratio of the two components of binary alloys. As far as we know, the shape, size and density of grains play important roles in optimizing catalytic, optical, transport and magnetic properties of nanostructural composite materials in comparison with bulk counterparts. Therefore, a number of theorists and experimentalists have put great efforts in controlling the morphology of the bimetallic nanoscale system in recent years. In particular, alloyed nanoparticles with hollow framework exhibit great advantages including much lower density and material cost and higher specific surface and permeability

*Corresponding author. Tel.: +86 10 82649159; fax: +86 10 82649531.
**Corresponding author. Tel.: +86 10 82339567; fax: +86 10 82317935.
E-mail addresses: rcyu@aphy.iphy.ac.cn (R. Yu), rmwang@buaa.edu.cn (R. Wang).

Peer review under responsibility of Chinese Materials Research Society.

Production and hosting by Elsevier

1002-0071 © 2013 Chinese Materials Research Society. Production and hosting by Elsevier B.V. All rights reserved.
http://dx.doi.org/10.1016/j.pnsc.2013.06.011

in comparison with their solid counterparts [8–10]. Among numerous candidates, hollow platinum based bimetallic nanospheres have aroused considerable research for their multiple functional roles played in catalysis [11–13]. On one hand, in light of the oxygen reduction phenomenon, a number of experiments have been carried out to examine the improved electrocatalytic activity and stability on the surfaces of nanoscale platinum bimetallic alloys. On the other hand, the catalytic characteristic of hollow nanospheres could also be tuned smartly by different synthesis routes which result in the discrepancy in microscopic architectures.

Since Vasquez et al. [14] and Sun et al. [15] first reported the synthesis of $Co_{58}Pt_{42}$ and $Ni_{30}Pt_{70}$ (using an average stoichiometry) hollow nanospheres with controlled morphology and composition respectively, their technological route has been used for synthesizing platinum based bimetallic hollow nanomaterials, which have a wide range of practical applications. For example, CoPt hollow nanospheres have been applied as perpendicular magnetic recording mediums in data storage industry [16] and NiPt has been used for improving catalytic efficiency in fuel cells and environmental chemistry [15]. As is well known, some industrial devices are sometimes operated at extreme conditions of high temperature and/or high pressure. So it is meaningful to study the structural stability of CoPt and NiPt hollow nanospheres under external pressure. However, up to now, the structural stability behavior of these platinum based bimetallic hollow nanomaterials under high pressure still remains uncertain. Consequently, in this work we report their structural behavior with pressure as a tunable thermodynamic parameter [17] by using *in situ* high pressure angle dispersive x-ray diffraction (ADXD) and Raman scattering measurements. In addition, we compare their bulk moduli obtained from experiments with the calculated ones.

2. Experimental procedure

The CoPt and NiPt hollow nanosphere samples were prepared by the general one-pot procedure without using a sacrificial template. The synthesis details on high quality hollow nanospheres were described elsewhere [15]. *In situ* high-pressure ADXD experiments of CoPt and NiPt were performed with a diamond anvil cell (DAC) for generating external pressure at room temperature by using synchrotron radiation source at 4W2 beamline of the Beijing Synchrotron Radiation Facility (BSRF, IHEP, Beijing) [18]. The spot size and wave length of the x-ray were 11 m × 32 m and 0.6199 Å, respectively. The culet of the DAC was 300 m in diameter and no pressure medium was utilized. The sample powder was loaded with the ruby as pressure calibration into a hole with 120 m in diameter in a T301 stainless steel gasket. The ratio V as a function of pressure P for the sample was obtained from the change of the spacing d between lattice planes got from

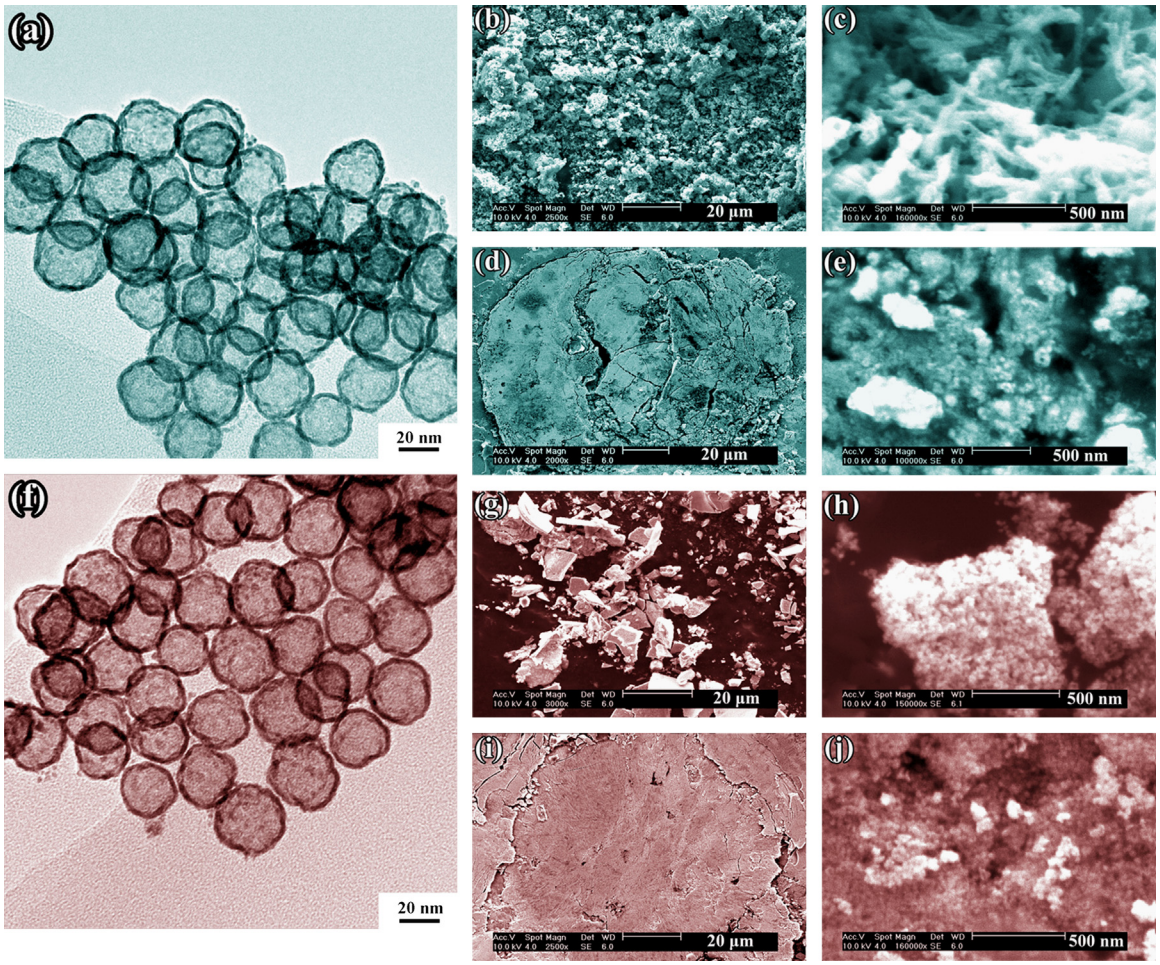

Fig. 1 TEM images and SEM micrographs of CoPt (a–e) and NiPt (f–j) hollow nanospheres: (a–c,f–h) before high pressure treatment; (d,e,i,j): after high pressure treatment.

the synchrotron radiation x-ray diffraction experiments. *In situ* high pressure Raman scattering experiments were conducted on a Renishaw Micro-Raman Spectroscopy System (inVia-Reflex).

Moreover, we calculated the bulk moduli of the materials relevant to CoPt and NiPt for comparison by using the Wien2k [19] packages. The morphology of the samples was characterized by using an FEI XL30 S-FEG scanning electron microscope (SEM).

3. Results and discussion

3.1. The morphology and in situ high-pressure ADXD experiments of CoPt and NiPt hollow nanospheres

The TEM images of CoPt and NiPt samples are shown in Fig. 1(a) and (f), respectively, which confirm the hollow nanosphere structure of these samples. Typical SEM micrographs of the as-synthesized CoPt and NiPt hollow nanospheres are presented in Fig. 1(b) and (c) and Fig. 1(g) and (h), respectively, corresponding to low and high magnification. They indicate clearly that both the nanomaterials represent spherical shape morphology with uniform grain size of about 50 nm despite of local aggregation of particles in needlelike for CoPt (Fig. 1(c)) and in cluster for NiPt (Fig. 1(h)). Fig. 1(d), (e), (i) and (j) shows the morphologies of CoPt and NiPt after high pressure processing in low and high magnification. Although both samples are compressed closely as bulk discoid shape from submicroscopic observation in Fig. 1(d) and (i) and there is a distinct change in microscopic morphology from Fig. 1(c), (e), (h) and (j), we can find that there is no remarkable discrepancy in grain size for the samples between before and after high-pressure treatment. Furthermore, the correlative energy-dispersive x-ray (EDX) spectra show that the average element ratios are close to Co:Pt=36:64 and Ni:Pt=39:61 for CoPt and NiPt hollow nanospheres, respectively.

Figs. 2 and 3(a) display the *in situ* ADXD patterns of CoPt and NiPt hollow nanospheres at different pressures up to ~41 GPa, respectively. At ambient pressure, both the nanospheres have a face centered cubic (*fcc*) structure with a space group of $\overline{3}Fmm$ and the lattice parameters are $a=0.39176$ and 0.38871 nm for CoPt and NiPt, respectively, this fact is consistent with the results of Sun et al. [15]. With increasing pressure up to ~41 GPa, no obvious change occurs in the diffraction patterns except for slight shifts of the peaks toward larger angle (as marked by arrows in Figs. 2 and 3(a)), this fact reveals the slight decrease of the lattice parameter. The weakening of the intensities of the sample peaks at high pressure is due to the sample flowage out of the sample cell in DAC, and slight broadening of the peaks is caused by the decrease of grain size and pressure gradients in the sample under high pressure. After releasing pressure to ambient environment (unloaded to 0.3 and 0.7 GPa for CoPt and NiPt, respectively), all the peaks of CoPt and NiPt nearly come back to the original sites as shown in Figs. 2 and 3(a). The unit cell volume at different pressures can be well derived from the refined lattice parameters and the pressure–temperature–volume dependence can be decided systematically by an appropriate equation of state. The Birch–Murnaghan (BM) equation [20,21] of the third order, being valid for the isotropic case in a quasi-hydrostatic pressure environment, is described as

$$P=\frac{3}{2}B_0\left[\left(\frac{V}{V_0}\right)^{-7/3}-\left(\frac{V}{V_0}\right)^{-5/3}\right]\left\{1-\frac{3}{4}(4-B_0')\left[\left(\frac{V}{V_0}\right)^{-2/3}-1\right]\right\}, \quad (1)$$

where V and V_0 represent the volumes of the unit cell at pressure P and ambient pressure, respectively, B_0 and B_0' are the isothermal

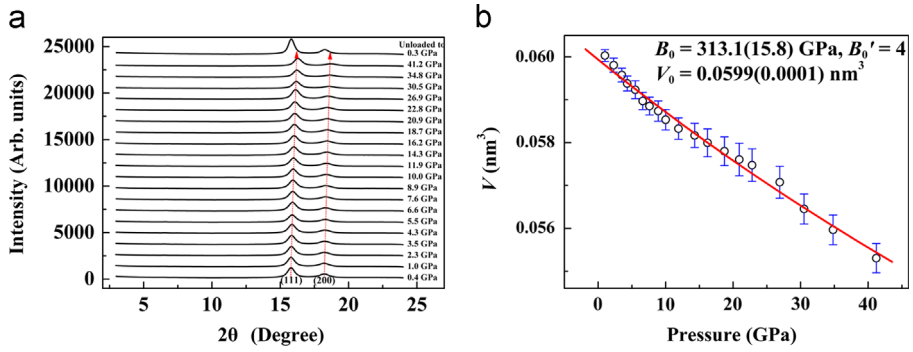

Fig. 2 ADXD patterns of the CoPt hollow nanospheres at different pressures and the unit cell volume as a function of pressure.

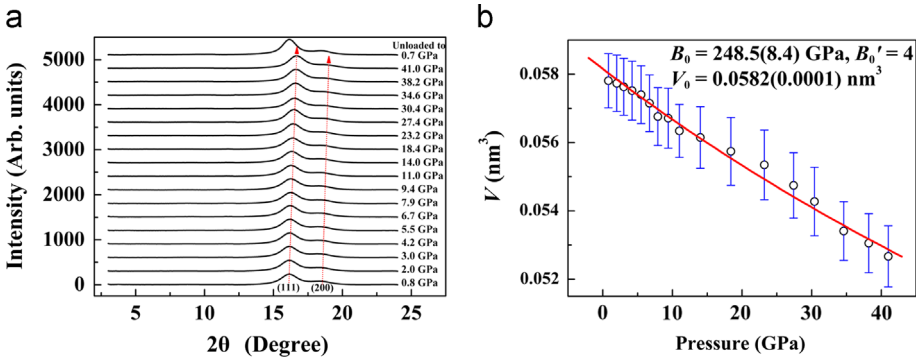

Fig. 3 ADXD patterns of NiPt hollow nanospheres at different pressures and the unit cell volume as a function of pressure.

bulk modulus and its first-order pressure derivative. Figs. 2 and 3 (b) show the pressure dependences of the unit cell volume for CoPt and NiPt hollow nanospheres, respectively, where the solid lines indicate the fitting curves with the BM equation of state and B_0' fixed as 4. We obtain the ambient pressure isothermal bulk moduli B_0=313.1(15.8) and 248.5(8.4) GPa for the CoPt and NiPt samples, respectively. In our measured pressure range, no crystal structural phase transition was observed in either CoPt or NiPt up to 41 GPa.

3.2. *The first-principles density functional theory calculations of Co–Pt and Ni–Pt*

In our case, the computer program Wien2k [19] was used not only to optimize crystal structure, but also to calculate the lattice constant and bulk modulus by considering the effect of magnetic moments. We performed the systematic first-principles density functional theory (DFT) calculations with PBE (J.P. Perdew, K. Burke and M. Ernzerhof) generalized gradient approximation (GGA) corrections [22]. In terms of the phase diagrams of Co–Pt and Ni–Pt alloys [23], we calculated the bulk moduli of relevant bulk materials by using structural information of Ni [24], Ni_3Pt_1 [25], Ni_1Pt_1 [23], Ni_1Pt_3 [25], Pt [26], and Co [27], respectively, and they are in well agreement with the previous reported results [28–30]. Besides, according to structural information of Co_3Pt_1 [31], Co_1Pt_1 [23], Co_1Pt_3 [31], we also calculated corresponding bulk moduli and showed the results in Fig. 4. With increasing mole concentration of platinum, other composition alloys retain cubic crystal symmetry except for the tetragonal Co_1Pt_1 and Ni_1Pt_1 [23] alloys. Moreover, Fig. 4 indicates all the calculated bulk moduli with solid circles for Co–Pt system and open squares for Ni–Pt system, where the dotted lines indicate the fitting curves showing the trend of change. Besides, it is worth to note that the experimentally obtained bulk moduli marked with solid and open asterisks for CoPt and NiPt in Fig. 4 are remarkably larger than the calculated ones, revealing that our hollow nanospheres are more difficult to compress than the corresponding bulk materials due to the small size effect associated with peculiar hollow nanostructure. Generally, nanometer materials like nanospheres have considerable surface and thus store much higher surface energy than the corresponding bulk materials. Hence, it is

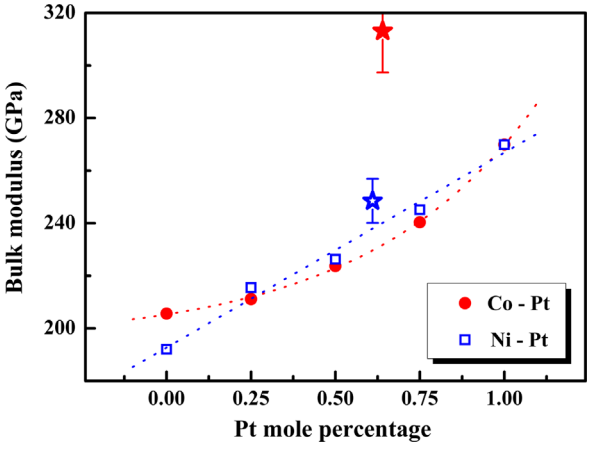

Fig. 4 The bulk modulus dependences of Co–Pt and Ni–Pt alloys with different Pt contents. Solid and open asterisks indicate the experimental bulk moduli of CoPt and NiPt, respectively.

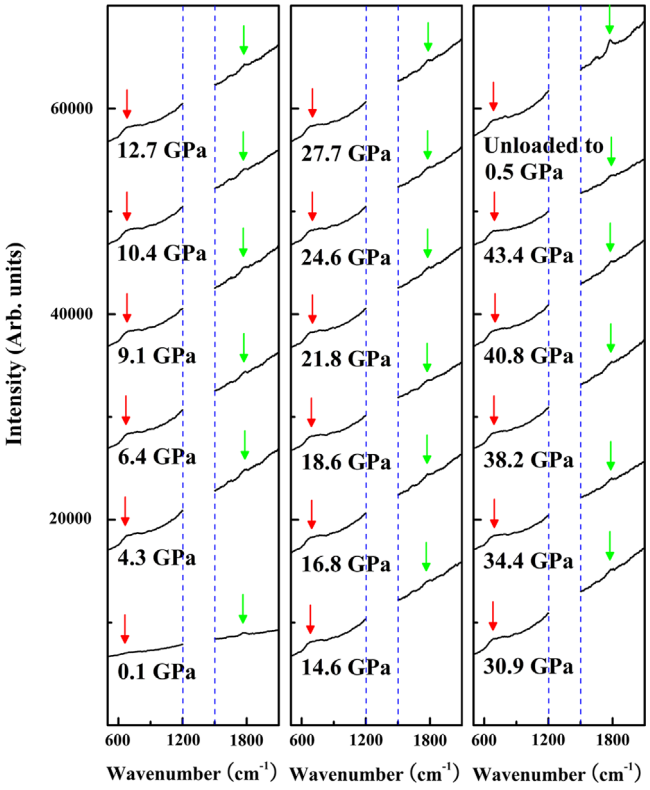

Fig. 5 High-pressure Raman scattering spectra of CoPt hollow nanospheres.

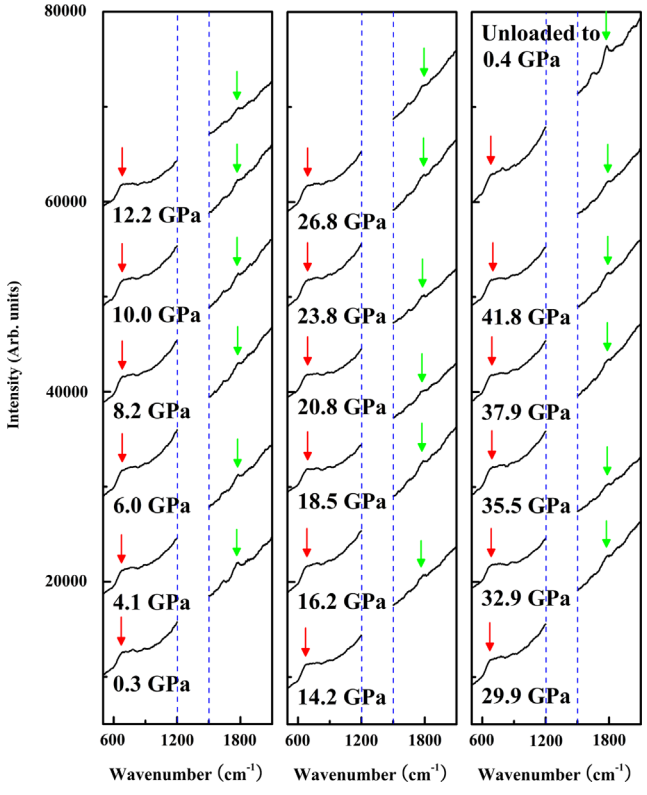

Fig. 6 High-pressure Raman scattering spectra of NiPt hollow nanospheres.

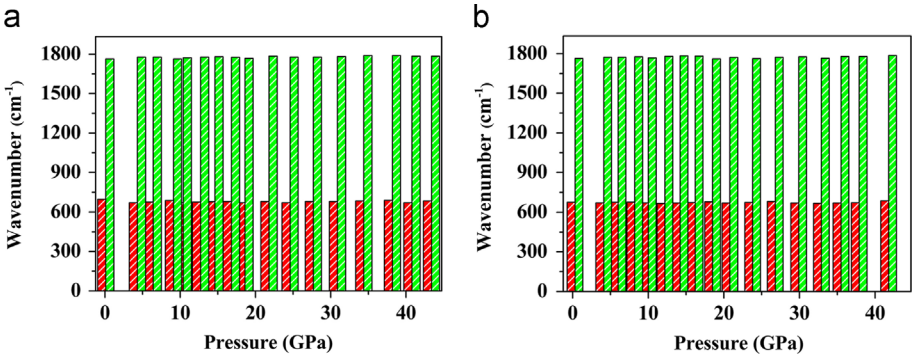

Fig. 7 The wavenumber dependences of pressure for CoPt and NiPt hollow nanospheres.

easy to understand that both CoPt and NiPt hollow nanospheres possess higher bulk moduli than their bulk counterparts.

3.3. In situ high pressure Raman scattering investigations of CoPt and NiPt hollow nanospheres

Raman scattering is a powerful tool for exploring structural changes of materials. Figs. 5 and 6 show the Raman spectra of CoPt and NiPt hollow nanospheres at different pressures up to ~43.4 GPa and ~41.8 GPa, respectively. All experimental data were collected discontinuously at each pressure point for avoiding the effect of Raman characteristic peak of diamond at 1332 nm^{-1}. As we know, the infrared radiation properties of centrosymmetric molecule CoPt and NiPt were studied in the past few years [32,33]. According to the well known mutual exclusion rule, CoPt and NiPt should not display any Raman activity at ambient pressure. So far, although we cannot find any report about their Raman properties, we indeed observe weak Raman activity happening in CoPt and NiPt hollow nanospheres as shown in Figs. 5 and 6, respectively, where the two weak Raman active vibrational modes at 697 and 1764 nm^{-1} for CoPt and at 676 and 1764 cm^{-1} for NiPt are marked by arrows at ambient pressure. It is likely from the break of centrosymmety, which may be induced by crystal structural distortion on the outer and/or inner surfaces of the peculiar hollow nanostructure. Besides this, the broadening of the Raman peaks is also a common feature of nanoscale materials.

Fig. 7 presents the positions of Raman characteristic peaks of CoPt and NiPt hollow nanospheres at different pressures and room temperature, respectively. With increasing pressure, we can identify that no distinguishable change in the wavenumbers for the two modes, revealing the sturdy of the Raman active vibrational modes on surface of hollow nanospheres with pressure. Consistent with the high pressure ADXD studies, the high pressure Raman scattering results also show nanocrystal structural transition in the two samples.

4. Conclusions

The *in situ* high-pressure ADXD and Raman experiments were performed for CoPt and NiPt hollow nanospheres at ambient temperature. Both experiments indicate that no crystal structural transition occurs in the measured pressure range. In terms of the BM equation of state, we obtain the ambient pressure isothermal bulk moduli B_0=313.1(15.8) and 248.5(8.4) GPa for the CoPt and NiPt nanospheres, respectively. Specially, we observe Raman activity happening in CoPt and NiPt hollow nanospheres due to the possible break of centrosymmetry, which may be induced by crystal structural distortion on the outer and/or inner surfaces of the peculiar hollow nanostructure. Besides, using first-principles DFT, we show that our hollow nanospheres possess higher bulk moduli than their bulk counterparts.

Acknowledgments

This work is supported by the State Key Development Program for Basic Research of China (Grant no. 2012CB932302), the National Natural Science Foundation of China (Grant no. 11174023) and Beijing Municipal Research Project for outstanding doctoral thesis supervisors (Grant no. 20121000603).

References

[1] J.L. Fernández, D.A. Walsh, A.J. Bard, Journal of the American Chemical Society 127 (2005) 357–365.
[2] R.W.J. Scott, O.M. Wilson, S.-K. Oh, E.A. Kenik, R.M. Crooks, Journal of the American Chemical Society 126 (2004) 15583–15591.
[3] H. Lang, S. Maldonado, K.J. Stevenson, B.D. Chandler, Journal of the American Chemical Society 126 (2004) 12949–12956.
[4] P. Mulvaney, Langmuir 12 (1996) 788–800.
[5] Z.J. Liang, A. Susha, F. Caruso, Chemistry of Materials 15 (2003) 3176–3183.
[6] D.H. Wan, H.L. Chen, S.C. Tseng, L.A. Wang, Y.P. Chen, ACS Nano 4 (2010) 165–173.
[7] S.H. Sun, C.B. Murray, D. Weller, L. Folks, A. Moser, Science 287 (2000) 1989–1992.
[8] X.W. Lou, L.A. Archer, Z.C. Yang, Advanced Materials 20 (2008) 3987–4019.
[9] J. Zeng, J.L. Huang, W. Lu, X.P. Wang, B. Wang, S.Y. Zhang, J.G. Hou, Advanced Materials 19 (2007) 2172–2176.
[10] H.P. Liang, H.M. Zhang, J.S. Hu, Y.G. Guo, L.J. Wan, C.L. Bai, Angewandte Chemie International Edition 43 (2004) 1540–1543.
[11] V.R. Stamenkovic, B.S. Mun, M. Arenz, K.J.J. Mayrhofer, C.A. Lucas, G.F. Wang, P.N. Ross, N.M. Markovic, Nature Materials 6 (2007) 241–247.
[12] S. Alayoglu, P. Zavalij, B. Eichhorn, Q. Wang, A.I. Frenkel, P. Chupas, ACS Nano 3 (2009) 3127–3137.
[13] R.M. Wang, H.Z. Zhang, M. Farle, C. Kisielowski, Nanoscale 1 (2009) 276–279.
[14] Y. Vasquez, A.K. Sra, R.E. Schaak, Journal of the American Chemical Society 127 (2005) 12504–12505.
[15] Q. Sun, Z. Ren, R.M. Wang, N. Wang, X. Cao, Journal of Materials Chemistry 21 (2011) 1925–1930.
[16] D.M. Newman, M.L. Wears, M. Jollie, D. Choo, Nanotechnology 18 (2007) 205301–205309.

[17] R.C. Yu, P. Zhao, F.Y. Li, Z.X. Liu, J. Liu, C.Q. Jin, Physical Review B 69 (2004) 214401–214405.
[18] J. Liu, J. Zhao, R.Z. Che, Y. Yang, Chinese Science Bulletin 45 (2000) 1659–1662.
[19] P. Blaha, K. Schwarz, G.K.H. Madsen, D. Kvasnicka, J. Luitz, WIEN2K, in: Karlheinz Schwarz (Ed.), Techn. Universitat, Wien, Austria, 2001.
[20] F. Birch, Journal of Geophysical Research 57 (1952) 227–286.
[21] F.D. Murnaghan, Proceedings of the National Academy of Sciences USA 30 (1944) 244–247.
[22] J.P. Perdew, K. Burke, M. Ernzerhof, Physical Review Letters 77 (1996) 3865–3868.
[23] C. Leroux, M.C. Cadeville, V. Pierron-Bohnes, G. Inden, H. Hinz, Journal of Physics F: Metal Physics 18 (1988) 2033–2051.
[24] E.R. Jette, F. Foote, Journal of Chemical Physics 3 (1935) 605–616.
[25] A. Kussmann, H.E. von Steinwehr, Zeitschrift für Metallkunde 40 (1949) 263–266.
[26] J.W. Edwards, R. Speiser, H.L. Johnston, Journal of Applied Physics 22 (1951) 424–428.
[27] A. Taylor, R.W. Floyd, Acta Crystallographica 3 (1950) 285–289.
[28] G. Bozzolo, H.O. Mosca, M.F. del Grosso, Intermetallics 16 (2008) 668–675.
[29] D. Paudyal, A. Mookerjee, International Journal of Modern Physics B 17 (2003) 4447–4456.
[30] G.Y. Guo, H.H. Wang, Chinese Journal of Physics 38 (2000) 949–961.
[31] A.H. Geisler, D.L. Martin, Journal of Applied Physics 23 (1952) 375.
[32] P. Podsiadlo, G. Krylova, B. Lee, K. Critchley, D.J. Gosztola, D.V. Talapin, P.D. Ashby, E.V. Shevchenko, Journal of the American Chemical Society 132 (2010) 8953–8960.
[33] H.M. Song, P.D. Ye, A. Ivanisevic, Langmuir 23 (2007) 9472–9480.